Transactions of the SMiRT 27
Yokohama, Japan, March 3-8, 2024
Division V

NUMERICAL AND THEORETICAL STUDY ON DYNAMIC FLEXURAL RESPONSES OF RC SLAB UNDER SOFT MISSILE IMPACT

Pengcheng Jia[1], Hao Wu[2], and Yuehua Cheng[3]

[1] Doctoral Student, Tongji University, Shanghai, China (pengchengjia@tongji.edu.cn)
[2] Professor, Tongji University, Shanghai, China (wuhaocivil@tongji.edu.cn)
[3] Postdoctoral Scholar, Tongji University, Shanghai, China (yhcheng@tongji.edu.cn)

ABSTRACT

Reinforced concrete (RC) slab is a common component to protect the nuclear facilities in plants' structures. Soft missile impacting RC slab is a potential scenario in aircraft impact and wind-induced missile accidents. Thus, the dynamic flexural responses of RC slabs against soft missile impact are studied numerically and theoretically in this paper. Firstly, the numerical simulation approach is validated by an existing soft missile impact test. Then, the influences of the missile's weight, impact velocity and diameter-thickness ratio for the concrete damage and dynamic flexural responses of RC slabs are further analysed by numerical simulation. The reliability of the Riera formula is verified by comparing it with the simulated impact force-time histories. Finally, the dynamic flexural resistance function of the RC slab and the single degree of freedom (SDOF) model for the soft missile impacting are established and validated by tests and numerical simulation results. It derives that: (i) the concrete scabbing and dynamic responses are sensitive to the impact velocity or diameter-thickness ratio increases in soft missile impact scenarios instead of the missile mass; (ii) the present SDOF model can be used to predict the soft missile impact responses of RC slabs against and assist to corresponding structural design.

INTRODUCTION

Reinforced concrete (RC) slabs are widely used as structural components in nuclear power plants (NPPs) and need to withstand various types of loads, such as static, dynamic, thermal, and blast. One of the extreme loading scenarios that may pose a threat to the integrity and safety of reinforced concrete slabs is the impact of a soft missile, such as an aircraft, a vehicle or steel tube (wind-borne missiles). The soft missile is characterized by low stiffness and high velocity, which could cause severe flexural damage to the NPP structures (Zhang et al. (2017), Zou et al. (2019)). Therefore, the flexural behaviour of RC slabs under soft missile impact is valuable for the structural design and evaluation of NPP structures.

To evaluate the behaviour of RC structures under various forms of impact loading, VTT has conducted testing as part of the IMPACT international projects, which have been jointly funded since 2005. The IMPACT projects have included soft impact testing, as an essential part of their experimental program, which provides reference data for validation of the numerical simulation approach. However, considering the limitations of modelling and computational efficiency, numerical simulation is suitable to reveal the action mechanism but inconvenient to apply directly to structural design. The lack of theoretical methods for soft missile-impacting RC slabs in existing studies limits the development of structural impact-resistant design.

In this paper, the influences of impact velocity, missile mass, and soft missile (steel tube) thickness on dynamic flexural behaviours of RC slabs subjected to soft impact loadings are first analysed by numerical simulation methods. Then, the application of the Riera function to soft impact load is tested by the above simulation results. Finally, a simplified single degree of freedom (SDOF) theoretical model is established to predict the dynamic flexural responses of RC slabs subjected to soft missile impact loadings.

NUMERICAL SIMULATION ANALYSIS

Based on the commercial software LS-DYNA, a numerical simulation method for soft missile impact is presented and validated by replicating the soft impact RC slab test conducted by Vepsä et al. (2012). Subsequently, this study further analyses the dynamic flexural response of the RC slab, focusing on the impact velocity, missile mass, and the soft missile's diameter-thickness ratio.

Analysis methods

In the numerical simulation, the soft missile's impact velocity is set by the keyword *INITIAL_ VELOCITY_GENERATION. All components, excluding the steel rebars and missile, are modelled using constant stress solid elements. To prevent spurious mode deformation, the belytschko-bindaman hourglass control (QH=0.1) is implemented. Longitudinal reinforcements and stirrups are modelled using Hughes-Liu beam elements. The soft missile (steel tube) is represented using fully integrated shell elements. The interaction between different components is facilitated by the *CONTACT_AUTO_ SURFACE_TO_SURFACE keyword. A single surface contact is utilized in the missile to prevent steel tube buckling and folding. Additionally, perfect bonding between the steel rebars and concrete is achieved using *CONSTRAINED_LAGRANGE_IN_SOLID.

There are several concrete models for solid elements, such as the Pseudo tensor, K&C, Winfrith concrete, HJC, CSC, RHT, and CDPM models. The K&C, Winfrith concrete, and CSC models are commonly suitable to concrete structures under several impact loadings. The Winfrith concrete model does not incorporate post-peak softening in the compression of concrete and shear dilatancy effect. However, the CSC model can account for the modulus reduction of damaged concrete and includes separate tension/compression damage coefficients, which are not considered in the K&C model. The CSC model was recommended for analyzing the impact responses of NPP structures according to Li et al. (2022).

LS-DYNA includes three common steel models: Plastic Kinematic, Piecewise Linear Plastic, and Johnson-Cook. The parameter determination for Piecewise Linear Plastic and Johnson-Cook models is more complex than that of the Plastic Kinematic model. The dynamic behaviors of steel in this study is described using the Plastic Kinematic model, which incorporates the Cowper-Symonds model, as illustrated in Equation 1.

$$DIF_s = \frac{\sigma_d}{\sigma_s} = 1 + \left(\frac{\dot{\varepsilon}}{C} \right)^{1/P} \tag{1}$$

where DIF_s is the dynamic increase factor with strain rate $\dot{\varepsilon}$. The dynamic stress (σ_d) and static stress (σ_s) of steel are related to the material parameters C and P. Stouffer and Dame (1996) recommend C and P values of 40.4 and 5 for mild steel, and 100 and 10 for stainless steel.

Model validation

The IRIS 2010 soft missile impact test was utilized by Vepsä et al. (2012) to validate the application of the numerical simulation analysis methods. In the test, a soft missile was utilized, which was a hollow stainless-steel tube with dimensions of 2111 mm in length and 256 mm in diameter. The missile weighed 50.5 kg and had an initial velocity of 110.2 m/s upon impact. The RC slab used in the test had dimensions of 2082mm×2082mm×150mm and was supported by a steel frame and rollers with clear spans of 2000 mm in both directions. The longitudinal reinforcement ratio for each direction and face was 0.2%, and the stirrup reinforcement ratio was 0.44%. The compressive strength of concrete was 63.9 MPa; the yield strengths of reinforcements (steel rebars) and stainless steel were 661.7 MPa and 304 MPa, respectively. The model parameters of concrete and steel are presented in Table 1. The finite element model, as shown in Figure 1, defined the RC slab boundary with nine steel rollers. The element erosion algorithm was employed to simulate the concrete scabbing, and the erosion criterion in the CSC model was the maximum principal strain and damage factor, with critical values of 0.1 and 1, respectively.

Table 1: Model parameters of concrete and steel (unit: t, mm, s)

Concrete (CSC model)								
Parameter	IRATE	ERODE	RECOV	G	K	ALPHA	THETA	LAMDA
Magnitude	1	1.1	11	14666	19555	21.5	0.335	13.5
Parameter	BETA	ALPHA1	THETA1	LAMDA1	BETA1	ALPHA2	THETA2	LAMDA2
Magnitude	0.0144	0.82	0	0.241	0.0064	0.76	0	0.16
Parameter	BETA2	R	X0	W	D1	D2	B	GFC
Magnitude	0.0055	1.97	138	0.065	6.1×10^{-4}	2.2×10^{-6}	20	7.19
Parameter	D	GFT	GFS	PWRC	PWRT	PMOD	ETA0C	NC
Magnitude	0.1	0.142	0.142	5	1	4.8	4.4×10^{-4}	0.78
Parameter	ETA0T	NT	OVERC	OVERT	SRATE	REPOW		
Magnitude	7.8×10^{-6}	0.36	50	50	1	1		
Steel rebars (Plastic Kinematic model)								
Parameter	E	SIGY	ETAN	SRC	SRP	FS		
Magnitude	200000	661.7	544	40.4	5	0.15		
Stainless steel (Plastic Kinematic model)								
Parameter	E	SIGY	ETAN	SRC	SRP	FS		
Magnitude	200000	304	584	100	10	0.5		

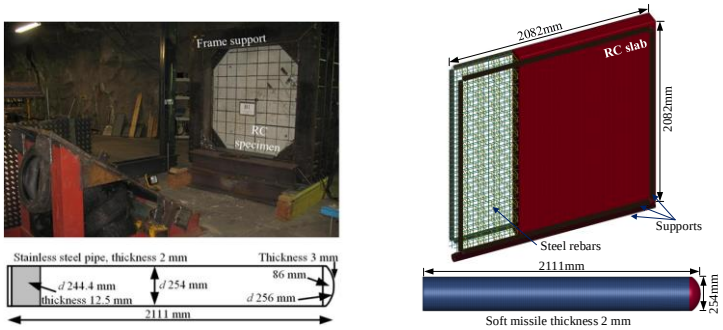

Figure 1. Soft missile impact test (a) test setup (b) finite element model

Figures 2 and 3 compares the soft missile deformation, concrete damage and measured deflection-time histories between the simulated and experimental results. The numerical simulation agrees with the test data in terms of the crushed and residual lengths of the soft missile, as shown in Figure 2(a). The numerical concrete damage is identical to experimental results. Moreover, the measured deflection-time histories in the numerical simulation closely match the corresponding test data, particularly the maximum deflection and natural vibration period of the RC slab.

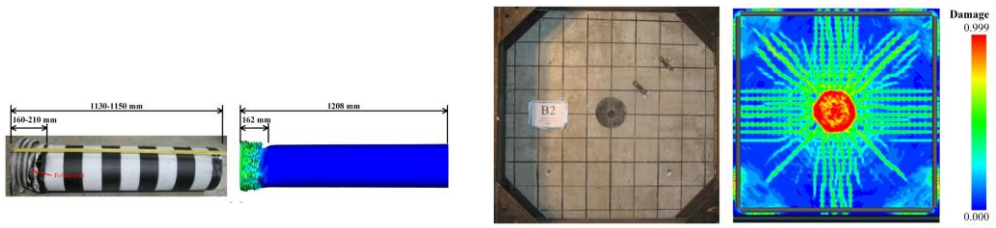

(a) (b)

Figure 2. Comparisons of damage (a) missile (b) RC slab (photos referred from Vepsä et al. (2012))

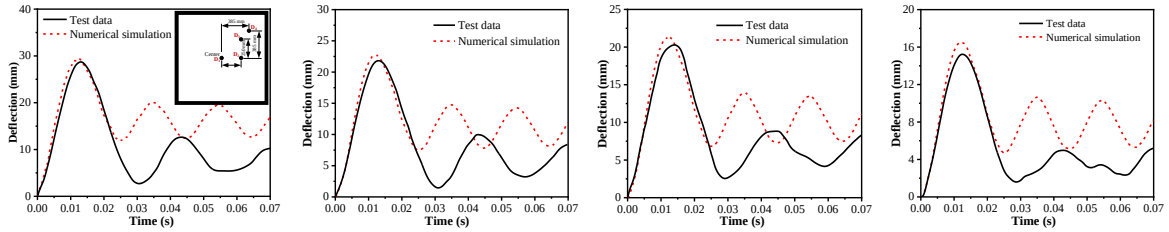

(a) (b) (c) (d)

Figure 3. Comparisons of the predicted deflection-time histories with test date from Vepsä et al. (2012) (a) D1 (b) D2 (c) D3 (d) D4

Parametric analyses

The parameter influence analyses are carried out using the validated analysis method. Figure 4 compares the concrete damage, impact force and central deflection of the RC slab under the soft missile impact with different velocity, mass and diameter-thickness ratio. Due to the buckling and crushing of the soft missile, the impact force-time history is oscillated in the numerical simulation and processed by 500Hz-Butterworth filtering. The comparisons in Figure 4 reveal the following findings: (i) The increase in impact velocity significantly exacerbates the back concrete damage of the slab, leading to concrete scabbing at an impact velocity of 150 m/s. The peak and duration of the impact force increase with the rise in impact velocity, and the change ratio of the maximum deflection is nearly the same as that of the impact energy. (ii) The increase in the mass of the soft missile has almost no effect on the distribution of the back concrete damage and the peak impact force. The duration of the impact force and the maximum deflection increase with the soft missile mass, but the increase level of the deflection is significantly lower than that of the impact energy caused by the mass increase. (iii) The decrease in the diameter-thickness ratio, i.e., an increase in the wall thickness, of the soft missile leads to back concrete damage (concrete scabbing), an increase in the peak impact force and the maximum deflection. However, it reduces the duration of the impact force. In conclusion, the impact condition with higher velocity results in more severe structural damage (scabbing and center deflection) under the same impact energy. Therefore, the structural impact-resistant design for the soft missile can be conducted with the maximum velocity under the same impact energy to ensure structural safety.

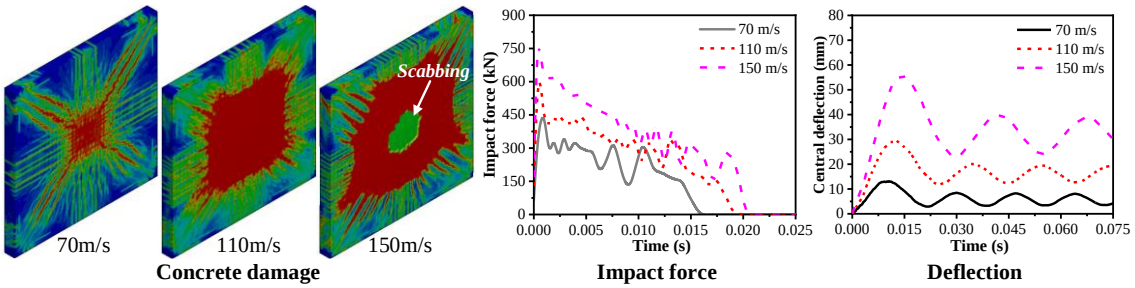

(a)

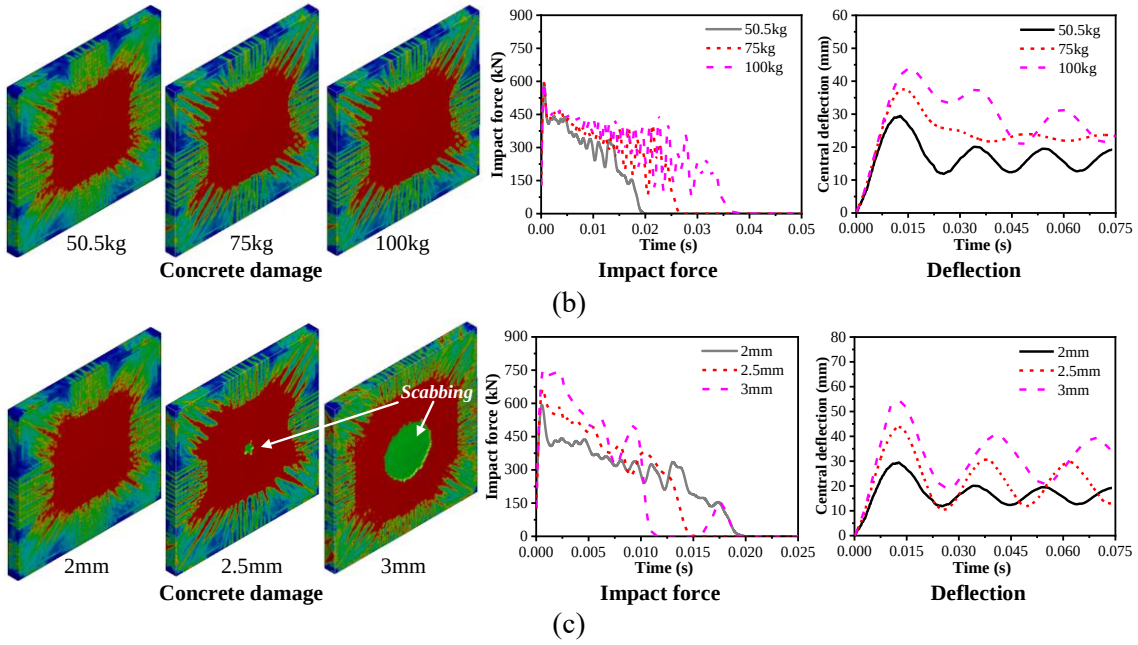

Figure 4. Parametric analyses for soft missile impacting RC slabs (a) impact velocity (b) missile mass (c) wall thickness of missile

THEORETICAL MODEL

The simplified theoretical model is established and verified in this section to assist the impact-resistant design of NPP structures.

Single Degree of Freedom model

The equivalent model is commonly employed to predict the dynamic flexural responses of structural members under dynamic loadings such as earthquakes, impacts, and blasts. In this study, the impact force can be obtained using the Riera function, and the RC slab is simplified as a one-degree-of-freedom model, as illustrated in Figure 5. The motion function of the SDOF model can be derived as Equation 2. Xiao et al. (2017) recommended that the slab's equivalent mass M_s is expressed as Equation 3.

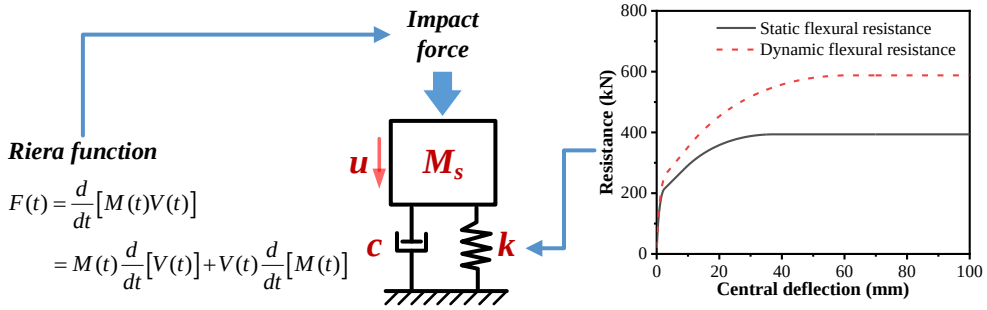

Figure 5. Establishment of the SDOF model

$$M_s\ddot{u}+c\dot{u}+ku=F(t) \tag{2}$$

$$M_s=\bar{m}_s\int_0^{2\pi}\int_0^{l/2}x\left[1-\frac{12x^2}{l^2}+\frac{16x^3}{l^3}\right]\mathrm{d}x\,\mathrm{d}\theta \tag{3}$$

where $\ddot{u}$, $\dot{u}$ and u represent the central acceleration, velocity, and displacement of the RC

slab, while $F(t)$ denotes the impact force-time history. The lateral stiffness k can be described by the dynamic flexural resistance function, and c represents the damping for global responses, with the damping ratio commonly assumed as 5% for RC slabs; $\bar{m}_s$ is the surface density; l are the clear span of the slab.

Impact force of soft missile

When the missile is deformable, a plastic shock assumption may be suitable, and a load-time function can be determined using simplified methods such as the Riera function (Riera, 1968). The impact process of a soft missile on a target depends on its momentum, i.e., $Ft=MV$, where F is the impact force, t is the time, M is the missile mass, and V is the impact velocity. The soft missile impact process lasts for a certain time. During this time, the force at any moment is equal to the change in the momentum of the missile in a very short time interval around that moment. This is assuming that the material of the target is compressed and does not bounce back. This differential form is derived from the original equation by dividing both sides by dt, as illustrated in Equation 4.

$$F(t)=\frac{d\left[M(t)V(t)\right]}{dt}=M(t)\frac{d[V(t)]}{dt}+V(t)\frac{d\left[M(t)\right]}{dt} \tag{4}$$

In Equation 4, the first term on the rightmost side represents the force that causes the mass M(t) of the uncrushed soft missile to decelerate, and it can be regarded as the crushing force of the soft missile, i.e., $P[x(t)]$. The second term on the rightmost side represents the inertial force of the crushed soft missile section at time t. Sugano et al. (1993) suggest introducing a reduction factor of less than 1 to the inertial force component of the Riera function based on impact tests. However, the reduction factor will result in the time integral of the impact force (i.e., impulse) being less than the missile's initial momentum. The reason they got the corresponding reduction factor might be the inapplicable $P[x(t)]$. For the steel tube, the crushing force is related to its length and diameter-thickness ratio. In this study, the corresponding $P[x(t)]$ can be derived by Equation 5 (Guillow et al. (2001)). The increase factor $DIF_{P[x]}$ caused by the strain rate effect is considered through Equation 6 (Lu and Yu (2003)).

$$P[x]=72.3\frac{f_y t^2}{2\sqrt{3}}\left(\frac{D}{t}\right)^{0.3} \tag{5}$$

$$DIF_{P[x]}=\left[1+\left(\frac{V_0}{2DC}\right)^{1/p}\right] \tag{6}$$

where f_y is the yield strength of wall material in the soft missile; t and D are the wall thickness and outer diameter of the missile, and V_0 is the initial impact velocity. Figure 6 compares the impact force-time history derived from the Riera function and the numerical simulation results. The Riera function calculated results agree well with numerical data in the peak impact force and duration, demonstrating its effectiveness for flexible structures. Thus, the Riera function can accurately capture the impact force-time history of the soft missile impacting RC slabs and can be used as a design tool for NPP structures.

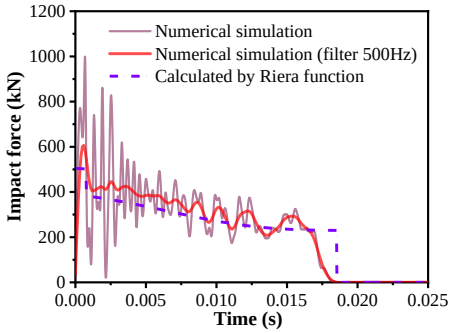

Figure 6. Impact force calculated by the Riera function

Dynamic flexural resistance function of RC slab

For the static flexural resistance function of RC slabs, Muttoni (2008) discovered that the main concentration of tangential crack and radial curvature of the RC slab is at the loading region. The radial curvature experiences a rapid decrease outside the critical crack radius r_0 as shown in Figure 7. Therefore, beyond r_0, the radial rotation could be considered as a constant ψ. The local deformation of the RC slab within the critical crack region can be approximated as spherical. The radial curvature χ_r and tangential curvature χ_t can be calculated using Equation 7.

$$\chi_t = \frac{\psi}{r},\ \chi_r = 0 \quad (r > r_0);\ \chi_t = \chi_r = \frac{\psi}{r_0} \quad (r < r_0),\ r_0 = r_c + H \tag{7}$$

where the critical shear crack denotes as r_c, and the radius of the loading region represents by r_0; H is the slab thickness. The force equilibrium of the slab strip is expressed as Equation 8, which can be utilized to derive the resistance function of RC slabs. The radial moment m_r and tangential moment m_t of the per-unit-width slab were expressed as the four-line moment-curvature function by Muttoni (2008), as illustrated in Figure 7(e). The flexural resistance (V_b) -rotation function of the RC slab can be derived by the moment balance, as shown in Figure 7(b) and Equation 9. The parameters in Equation 9 can be obtained from the specifications of RC slabs and Equations 10-12, as recommended by Muttoni (2008).

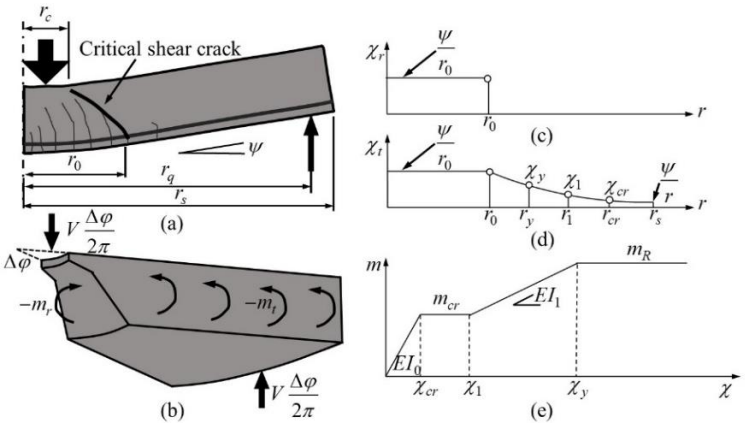

Figure 7. Assumptions of the slab strip: (a) geometry (b) internal forces (c) distribution of radial curvature. (d) distribution of tangential curvature (e) moment-curvature relationship

$$V\frac{\Delta\varphi}{2\pi}\left(r_q - r_c\right) = -m_r\Delta\varphi r_0 - \Delta\varphi\int_{r_0}^{r_s} m_t dr \tag{8}$$

$$V_b = \frac{2\pi}{r_q - r_c}\begin{pmatrix} -m_r r_0 + m_R\langle r_y - r_0\rangle + EI_1\psi\langle \ln(r_1) - \ln(r_y)\rangle + \\ EI_1\chi_{TS}\langle r_1 - r_y\rangle + m_{cr}\langle r_{cr} - r_1\rangle + EI_0\psi\langle \ln(r_s) - \ln(r_{cr})\rangle \end{pmatrix} \quad (9)$$

$$m_{cr} = \frac{f_t' H^2}{6},\quad EI_0 = \frac{E_c H^3}{12},\quad \chi_{cr} = \frac{m_{cr}}{EI_0} = \frac{2f_t'}{HE_c} \quad (10)$$

$$m_R = \rho f_y d^2\left(1 - \frac{\rho f_y}{2f_c'}\right),\quad EI_1 = \rho\beta_r E_s d^3\left(1 - \frac{c}{d}\right)\left(1 - \frac{c}{3d}\right),\quad c = \rho\beta_r\frac{E_s}{E_c}d\left(\sqrt{1 + \frac{2E_c}{\rho\beta_r E_s}} - 1\right) \quad (11)$$

$$\chi_{TS} = \frac{f_t'}{6H\rho\beta_r E_s},\quad \chi_1 = \frac{m_{cr}}{EI_1} - \chi_{TS},\quad \chi_y = \frac{m_R}{EI_1} - \chi_{TS},\quad r_1 = \frac{\psi}{\chi_1},\quad r_y = \frac{\psi}{\chi_y},\quad r_{cr} = \frac{\psi}{\chi_{cr}} \quad (12)$$

where $\Delta\varphi$ is the angle of the slab sector; ψ is the RC slab's support rotation in Figure 7(a); the operator $\langle x\rangle$ is x for $x\geq 0$ and 0 for $x<0$; E_s and f_y are the elastic modulus and yield strength of longitudinal reinforcements; EI_0 is the flexural stiffness of slabs without concrete crack; EI_1 is the flexural stiffness of slabs with concrete cracking; c is the compression zone depth; ρ and β_r are the ratio and efficiency factor of the longitudinal reinforcement, as well as the recommended β_r is 0.6 from Muttoni (2008); d is the effective thickness; m_{cr} and m_R are the cracking moment and nominal moment capacities of per unit-width slab; r_1, r_q, r_{cr}, r_y and r_s are the radius of stabilized cracking zone, the load introduction at the perimeter, cracked zone, yielded zone and circular isolated element, respectively; χ_1, χ_y, χ_{cr} and χ_{TS} are the curvature at stabilized cracking, yielding and cracking, as well as the decrease in curvature due to tension stiffening, respectively. To consider the strain rate effect of materials in the resistance function, the dynamic increase factors of concrete and steel are 1.2 and 1.5 respectively in this study.

Model verification

The central maximum deflection of RC slabs under soft missile impact loadings can be used as an important indicator for its damage assessment. Based on the prediction formula of the maximum deflection of the component by the SDOF model of the RC slab under the soft missile impact established above, the experiments conducted by Vepsä et al. (2012) and the numerical simulation conditions carried out in this paper are analyzed. It can be found that the SDOF model can better predict the deflection time history at the center of the plate in the experiment and the maximum deflection in the numerical simulation conditions. Most of the prediction results are within 20% error with the experimental or simulation results, which indicates the validity of the established SDOF model.

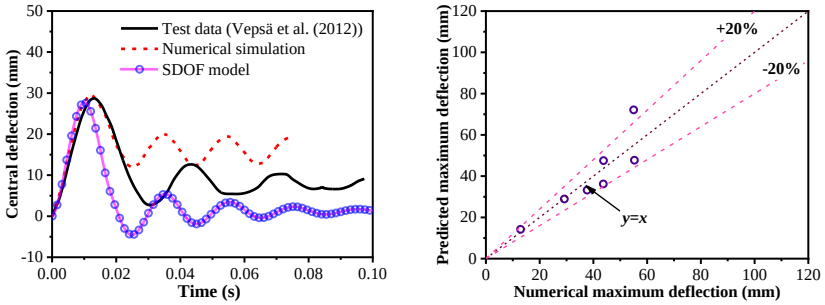

(a) (b)

Figure 8. Evaluation of the theoretical method (a) slab's central deflection-time histories (b) Predicted maximum deflection

CONCLUSION

This study carried out numerical simulation and theoretical analysis of soft missile impact on RC slab and revealed the influence laws of impact velocity, mass, and restitution coefficient of the soft missile on the dynamic behaviours of RC slabs. The results showed that the impact velocity and soft missile's diameter-thickness ratio of the soft missile had significant effects on the concrete damage and dynamic flexural responses of the RC slab, but the missile mass almost not change its damage distribution. Therefore, in structural impact-resistant design, the impact velocity and soft missile's diameter-thickness ratio should be paid more attention.

Based on the impact force-time history derived by the Riera function, this study further established an SDOF model of soft missile impact on RC slab and obtained the verification of experiment and numerical simulation. The present SDOF model can further assist the nuclear power plant structural design against soft missile impact.

REFERENCES

Guillow, S. R., Lu, G., Grzebieta, R. H., (2001). "Quasi-static axial compression of thin-walled circular aluminium tubes," *International Journal of Mechanical Sciences*, UK, 43(9) 2103-2123.

Li, Z. C., Jia, P. C., Jia, J. Y., Wu, H., Ma, L. L. (2022). "Impact-resistant design of RC slabs in nuclear power plant buildings," *Nuclear Engineering and Technology*, Republic of Korea, 54(10) 3745-3765.

Lu, G. and Yu, T.X. (2003) *Energy Absorption of Structures and Materials*, Woodhead Publishing Limited.

Muttoni, A. (2008). "Punching shear strength of reinforced concrete slabs without transverse reinforcement," *ACI Structural Journal*, USA, 105(2) 440-450.

Stouffer, D.C., Dame, L.T. (1996). *Inelastic deformation of metals: models, mechanical properties, and metallurgy*, John Wiley and Sons.

Sugano, T., Tsubota, H., Kasai, Y., Koshika, N., Orui, S., Von-Rieseman, W. A., Parks, M. B. (1993) "Full-scale aircraft impact test for evaluation of impact force," *Nuclear Engineering and Design*, UK, 140(3) 373-385.

Vepsä, A., Saarenheimo, A., Tarallo, F., Rambach, J., Orbovic, N. (2012). "Impact Tests for IRIS_2010 Benchmark Exercise," *Journal of Disaster Research*, Japan, 7(5) 619-628.

Zhang, T., Wu, H., Fang, Q., Huang, T. (2017) "Numerical simulations of nuclear power plant containment subjected to aircraft impact," *Nuclear Engineering and Design*, UK, 320: 207-221.

Zou, D., Sui, Y., Chen, K., Yu, X. (2019) "A cross‐scale refined damage evolution analysis of large commercial aircraft crashing into a nuclear power plant," *The Structural Design of Tall and Special Buildings*, UK, 28(16) e1668.